Early Intermediates in the Photocycle of the Glu46Gln Mutant of Photoactive Yellow Protein: Femtosecond Spectroscopy

Savitha Devanathan,* Su Lin,[†] Michael A. Cusanovich,* Neal Woodbury,[†] and Gordon Tollin*

*Department of Biochemistry, University of Arizona, Tucson, Arizona 85721; and [†]Department of Chemistry and Biochemistry, Arizona State University, Tempe, Arizona 85287 USA

ABSTRACT   Transient absorption spectroscopy in the time range from −1 ps to 4 ns, and over the wavelength range from 420 to 550 nm, was applied to the Glu46Gln mutant of the photoactive yellow protein (PYP) from *Ectothiorhodospira halophila*. This has allowed us to elucidate the kinetic constants of excited state formation and decay and photochemical product formation, and the spectral characteristics of stimulated emission and the early photocycle intermediates. Both the quantum efficiency (~0.5) and the rate constants for excited state decay and the formation of the initial photochemical intermediate (I_0) were found to be quite similar to those obtained for wild-type PYP. In contrast, the rate constants for the formation of the subsequent photocycle intermediates ($I_0^{\ddagger}$ and I_1), as well as for I_2 and for ground state regeneration as determined in earlier studies, were found to be from 3- to 30-fold larger. The structural implications of these results are discussed.

INTRODUCTION

The bacterial photoreceptor photoactive yellow protein (PYP) from *Ectothiorhodospira halophila* (Meyer, 1985; Meyer et al., 1987, 1989) utilizes a thiol ester-linked *p*-hydroxycinnamoyl chromophore as a light-transducing element (Baca et al., 1994; Hoff et al., 1994a). PYP has been suggested to control phototactic responses of this organism (Sprenger et al., 1993). A PYP amino terminal domain has recently been shown to control the expression of the gene for chalcone synthase in *Rhodospirillum centenum*, via a C-terminal histidine kinase domain of a phytochrome analogue (Jiang et al., 1999).

Absorption of a light photon (λ_{max} = 446 nm) by PYP induces a photocycle consisting of a series of transient intermediates, with lifetimes ranging from subpicoseconds to milliseconds (Meyer et al., 1987, 1991; Hoff et al., 1994b; Ujj et al., 1998; Devanathan et al., 1999). Picosecond (Ujj et al., 1998) and femtosecond (Devanathan et al., 1999) time-resolved spectroscopy have recently been used to obtain new insights into the cascade of early events following photon absorption by wild-type (WT) PYP. These studies have identified two new early red-shifted intermediates, I_0 and $I_0^{\ddagger}$, in addition to the previously known microsecond (I_1) and millisecond (I_2) intermediates, and have resolved the kinetics of the conversion of $I_0^{\ddagger}$ to the less red-shifted I_1 species. We have now extended the femtosecond experiments to include a site-specific mutant modified at Glu46, an important PYP color-regulating residue located in the active site. It has previously been shown (Genick et al., 1997; Mihara et al., 1997) that when Glu46 was mutated

to Gln, the PYP absorption spectrum was red-shifted by 16 nm, due to alteration of the H-bonding interaction between the Glu46 carboxyl group and the phenolate oxygen of the chromophore (Borgstahl et al., 1995; Xie et al., 1996). Furthermore, the photocycle kinetics for the mutant were also significantly altered, with time constants which were ~5 times faster for the I_1 to I_2 transition (τ = 53 μs) and ~3 times faster for the I_2 to P recovery process (τ = 50 ms) in comparison to WT protein (Genick et al., 1997). As will be demonstrated below, the time constants for the formation of I_1 and $I_0^{\ddagger}$ are also significantly decreased by this mutation, whereas the time constant for the formation of the initial photochemical intermediate (I_0) is relatively unaffected, as is the quantum efficiency for the conversion of the excited state into I_0. The structural basis of these results is discussed. This is the first report of the early time events in the photocycle of a PYP mutant.

EXPERIMENTAL

Sample preparation

Glu46Gln was prepared as reported previously (Genick et al., 1997) and was a generous gift from Dr. E. Getzoff's laboratory (Scripps Research Institute, La Jolla, Ca). Four milliliters of Glu46Gln-PYP solution (1.4 OD/ml) in 20 mM Tris-Cl buffer at pH 7.0 was used in the sample wheel of the femtosecond spectrometer, which had an optical pathlength of 2 mm and a radius of 10 cm, and was rotated at 5 Hz during data collection. Excitation was at 467 nm. Data were collected at ambient temperature.

Instrumental setup

Time-resolved absorption difference spectra were recorded on a femtosecond transient spectrometer described previously (Devanathan et al., 1999). Briefly, the apparatus consists of a pulsed laser and a pump-probe optical setup. The laser pulses were provided by a Ti:S regenerative amplifier (Model CPA-1000, Clark-MXR, Dexter, MI) pumped by a diode-pumped solid state laser (Model Millenia V, Spectra Physics, Mountain View, CA). The output of the CPA-1000 was 900 mW at 790 nm, with a 1 KHz repetition rate. Most of the CPA output (80%) was used to pump a modified optical parametric amplifier (Model IR-OPA, Clark-MXR) to

generate excitation at 467 nm. The rest of the laser output was focused onto a 1 cm flowing water cell to generate a white light continuum, which was further split into two identical parts used as probe and reference beams. The probe and reference signals were focused into two separate optical fibers coupled with a dual diode array detector (Model DPDA-1024, Princeton Instruments, Trenton, NJ). Excitation energy at the sample was adjusted to approximately 1 μJ per pulse using neutral density filters. The beam size at the sample was 0.5 mm in diameter. The polarization of the excitation beam was set at the magic angle (54.7°) relative to the probe and reference beams.

Data fitting

Data were analyzed in two different ways. First, nonlinear least-squares procedures, using an implementation of the Levenberg-Marquardt algorithm as incorporated into the Microcal Origin software package, were used to separately fit the dispersion-corrected kinetic data for the time regions between −1 and 6.5 ps, 10 and 500 ps, and 1 and 3.5 ns, using selected wavelengths in the spectral range of 410–550 nm. As described earlier (Ujj et al., 1998; Devanathan et al., 1999), a Gaussian cross-correlation function was used to represent the instrumental response corresponding to the pump-probe laser pulse. The cross-correlation time, which measures the temporal behavior of the pump-probe pulse widths and the fluctuation of the overlap between the two pulses, was found to be 0.5 ps over the entire measured spectral range. The decay kinetics in each of the above time ranges were fit with a single exponential term. Global kinetic fits were performed using selected transients within this spectral region. As shown previously (Ujj et al., 1998; Devanathan et al., 1999), the 420–460 nm region follows ground state bleaching and recovery, whereas the 470–550 nm region monitors stimulated emission and photochemical intermediate formation and decay.

The second analysis method involved fitting all of the data between −1 and 500 ps and from 420 to 540 nm globally to a series of exponential decay terms. Global fits of the data taken on the 4 ns time scale were also performed. The global fits were done using a locally written program (ASUFIT) based on MatLab (Mathworks, Natick, MA). In this case, dispersion correction was performed during the fit by altering the fitting function according to a separately measured dispersion correction curve (measured as in Devanathan et al., 1999). The results of these fits were used to construct the difference spectra of each of the kinetically resolved intermediates.

RESULTS

The transient absorbance spectra obtained during the first 10 ps after excitation of the Glu46Gln mutant (Fig. 1) clearly shows ground state bleaching and partial recovery at 440–480 nm, and stimulated emission in the 490–530 nm spectral region. These compare very well to the spectra obtained for WT-PYP (a representative example is also shown in Fig. 1), with the red-shift for all these processes correlating with the 16-nm shift between the mutant and WT-PYP ground state absorbance maxima (Genick et al., 1997). As was the case with WT-PYP, the partial ground state recovery indicates the formation of the I_0 intermediate. Furthermore, as shown by the 7.5 ps spectrum, disappearance of the stimulated emission and the appearance of a red-shifted photochemical intermediate is indicated by the positive absorbance in the 510–530 region. This latter species persists to longer times (see below), and is presumed to be the $I_0^{\ddagger}$ intermediate.
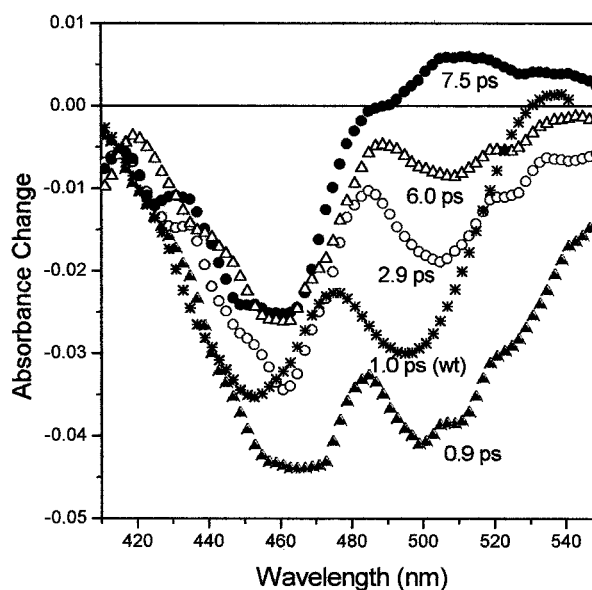

FIGURE 1 Transient spectra obtained at early times during excitation of the E46Q mutant of PYP. A spectrum obtained previously (Devanathan et al., 1999) for WT-PYP (*) is shown for comparison.

Kinetic traces at a variety of probe wavelengths have been analyzed for the three time ranges. For the −1 ps to 6.5 ps time window at short wavelengths (Fig. 2), ground state depletion, due to excited state formation after photon absorption, was observed as a negative difference signal appearing within a few hundred femtoseconds (within the time resolution of the instrument). This is similar to data previ-
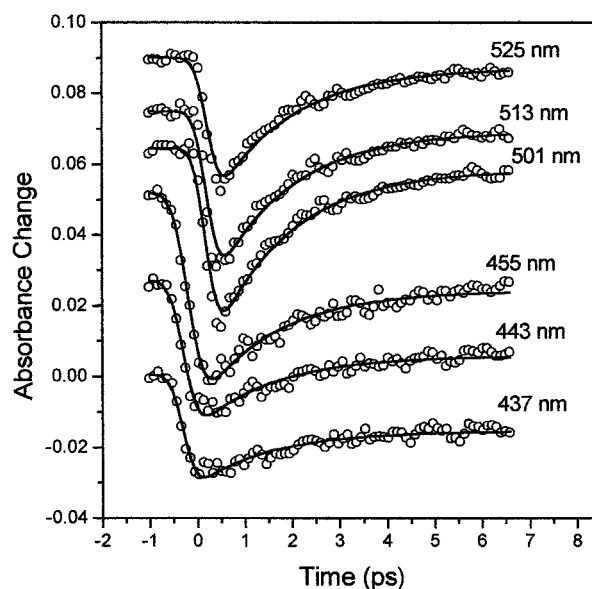

FIGURE 2 Kinetic transients obtained upon excitation of the E46Q mutant of PYP in the −1 to 6 ps time range. Baselines have been shifted for clarity. Solid lines through the data points correspond to global fits obtained as described in the text.

ously obtained for WT-PYP (Devanathan et al., 1999). As noted above, partial ground state recovery is indicative of the formation of at least one early photochemical intermediate. The decay of the excited state (as probed by stimulated emission) is seen in the long wavelength regions (480–525 nm; Fig. 2). Note that this decay is virtually complete by 6.5 ps.

Kinetic data obtained at longer times (10 ps to 100 ps; Fig. 3) show the formation of positive absorbance, which we ascribe to the previously identified $I_0^{\ddagger}$ intermediate. This species persists for as long as 500 ps (data not shown). Kinetic data obtained in the 1 ns to 3.5 ns time region show the decay of $I_0^{\ddagger}$ to form I_1 (Fig. 4).

Global nonlinear least-squares fits using selected wavelengths are represented by the solid lines in Figs. 2–4. For the fast time scale region shown in Fig. 2, the decay portions of the curve can be fit by a single exponential function using the same rate constant at all wavelengths ($k_{obs} = 0.63 \pm 0.05 \times 10^{12}$ s^{-1}). This value is similar to that obtained for the 460 nm excitation data with WT-PYP ($0.83 \pm 0.03 \times 10^{12}$ s^{-1}; Devanathan et al., 1999). In order to interpret the present results, we will use a similar kinetic model, shown in Fig. 5, which involves two competing processes:

(1) The repopulation of the ground state from the excited state, directly observed at 410–460 nm and indirectly observed as stimulated emission at 480–550 nm (rate constant, k_d) and

(2) The formation of the photochemical intermediate I_0, which occurs with a rate constant k_p.

According to this model, the relative amounts of the ground state P_{GS} and the intermediate I_0 produced from the
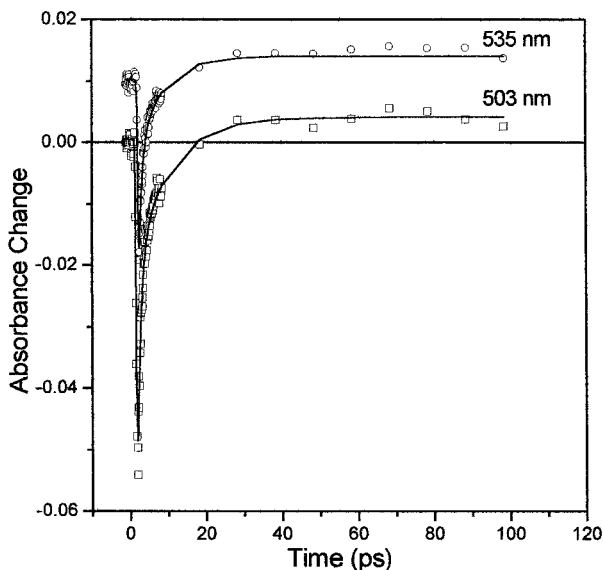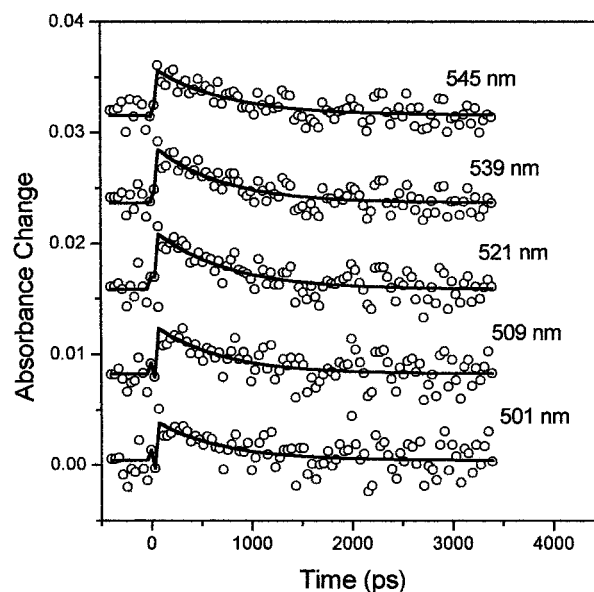

FIGURE 4 Kinetic transients obtained upon excitation of the E46Q mutant of PYP in the −1 ps to 3.5 ns time range. Baselines have been shifted for clarity. Solid lines through the data points correspond to global fits obtained using the same kinetic constants as in Fig. 3, plus an additional single exponential with a time constant of 680 ps.

excited state P* (quantum yield of photoproduct formation) will depend on the relative magnitudes of these two rate constants. Assuming no additional intermediates, $k_{obs} = k_d + k_p$, consistent with the single exponential decay obtained in both wavelength regions.

Deconvolution of the two rate constants from k_{obs} is straightforward. Based on our previous observation (Ujj et al., 1998) that I_0 does not have significant absorbance at the PYP ground state wavelength maximum, the extent of permanent bleaching of the ground state after excited state decay is complete can be calculated from the transient obtained at ~462 nm to be 54%. Note that this value for the quantum yield is very similar to that obtained in a similar manner (Devanathan et al., 1999) for WT-PYP (53%). This can be compared with values of 67% (Meyer et al., 1991)

FIGURE 3 Kinetic transients obtained upon excitation of the E46Q mutant of PYP in the −1 to 100 ps time range. Baselines have been shifted for clarity. Solid lines through the data points correspond to global fits obtained using the same kinetic constants as in Fig. 2 plus an additional single exponential with a time constant of 8 ps.
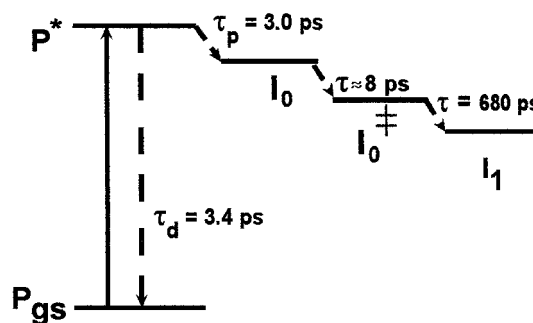

FIGURE 5 Scheme showing proposed mechanism of photoproduct formation in the E46Q mutant of PYP.

and 35% (Van Brederode et al., 1995) reported earlier for WT-PYP using different methodologies. Considering the errors involved in such measurements, the agreement is satisfactory. The partitioning of the excited state between the repopulation of the ground state and intermediate I_0 formation results in the following expression for the quantum yield: $\Phi = k_p/(k_p + k_d)$. Thus, from the observed quantum yield of product formation and the observed total decay rate constant, the individual rate constants can be calculated to be $k_d = 0.30 \times 10^{12}$ s^{-1} ($\tau = 3.4$ ps) and $k_p = 0.33 \times 10^{12}$ s^{-1} ($\tau = 3.0$ ps; Fig. 5). These values are similar to those obtained for WT-PYP ($\tau = 2.6$ ps and 2.3 ps, respectively; the small difference between these two values and those reported in Devanathan et al. (1999) is due to a calculation error). These results are consistent with the observation of Chosrowjan et al. (1998) that the fluorescence lifetime of the Glu46Gln mutant is similar to that of WT-PYP.

Global fits for kinetic traces in the time window from 10 ps to 100 ps for the long wavelength region (500–550 nm) were also performed. Although these data can be fit by a single exponential with a time constant $\tau = 8$ ps (k = $0.12 \pm 0.01 \times 10^{12}$ s^{-1}), the data are not of high enough quality to resolve the processes of stimulated emission decay and conversion of I_0 to $I_0^\ddagger$, which occur in the early part of this time domain. (Global fits of the data over the entire wavelength range were unable to statistically resolve two lifetimes on the subpicosecond time scale; see below.) Thus, this must be considered an approximate value. However, it is clear that $I_0^\ddagger$ formation occurs much faster (as much as 30 times faster) than observed with the WT protein (Devanathan et al., 1999). The decay of $I_0^\ddagger$ (Fig. 4) occurs according to a single exponential with a time constant $\tau = 680$ ps (k = $1.5 \pm 0.13 \times 10^9$ s^{-1}). Although the data are rather noisy, it is clear that this process also occurs faster (by as much as 5 times) than the corresponding step for WT-PYP (Devanathan et al., 1999). The Glu46Gln photocycle is shown in Fig. 6.

Fig. 7 shows the results of global exponential decay analyses over the entire wavelength range of the measurement (see Experimental section) and reconstruction of the P*, $I_0^\ddagger$ and I_1 difference absorbance spectra. The early decay processes (less than 20 ps) were modeled as a single decay (3.6 ps) and extrapolated back to zero time to generate the initial P* spectrum. (Statistically, the use of two exponential decays in the early time region was unwarranted, though the use of additional exponential terms did not change the resultant P* and $I_0^\ddagger$ spectra.) The $I_0^\ddagger$ difference absorbance spectrum was calculated as the spectral species remaining after the early time decay was complete in the 500 ps time scale data set. Finally, using the 4 ns data set, the spectral component with a constant amplitude on this time scale gave the absorbance difference spectrum of the I_1 state.
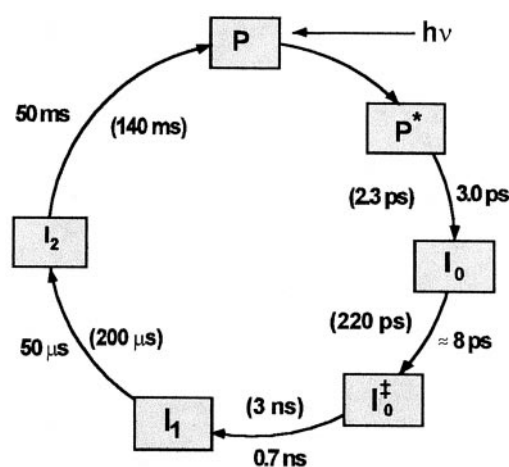

FIGURE 6 Photocycle of E46Q mutant of PYP. Values in parentheses correspond to time constants for WT-PYP.

In this analysis, we assume that the time scales for the two sequential reactions are sufficiently distinct that they can be modeled independently of one another. To a very good approximation this is true, as the $I_0^\ddagger$ state is formed in picoseconds, whereas the I_1 state requires hundreds of picoseconds to form. This being the case, the spectrum of the total amplitude of the fitting function at time 0 should represent the initial excited state, P*, the spectrum of the amplitude of the fitting function on the tens of picosecond time scale should be $I_0^\ddagger$ and the spectrum of the amplitude of the fitting function on the several nanosecond time scale should be the spectrum of I_1.

As might be expected, the difference spectrum of the initial excited state, P*, shows two negative features, one representing ground state bleaching centered near 460 nm (the small sharp peak in this region is a scattering artifact from the excitation beam) and another centered near 510 nm, which is the stimulated emission from the excited state. In the $I_0^\ddagger$ state, the ground state bleaching near 460 nm persists because the chromophore has not returned to its ground state, but the stimulated emission has disappeared, implying that the system is no longer in an excited singlet state. The stimulated emission band has been replaced by a broad absorbance increase above 485 nm characteristic of the $I_0^\ddagger$ intermediate (Ujj et al., 1998). Finally, formation of the I_1 state results in the disappearance of the long wavelength absorbance decrease, whereas the ground state bleaching of the chromophore remains. All of these spectra are consistent with the earlier results with WT-PYP (Ujj et al., 1998; Devanathan et al., 1999).

DISCUSSION

Optical excitation of the Glu46Gln mutant by femtosecond pulses results in the formation of a transient excited state (observed via ground state bleaching and stimulated emis-
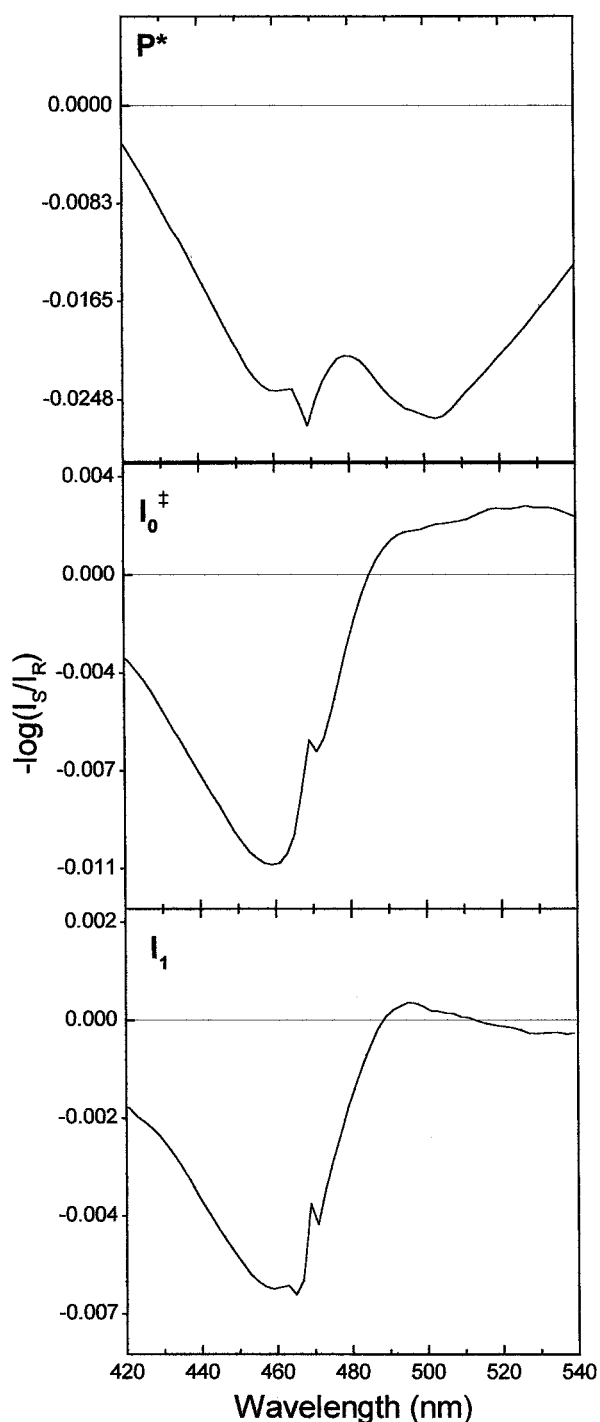
FIGURE 7 Difference spectra [plotted as $-\log (I_{Sample}/I_{Reference})$] calculated for P*, $I_0^{\ddagger}$ and I_1 from global exponential decay analysis. The P* spectrum (shown as ground state bleaching and stimulated emission) was calculated as the difference spectrum at zero time in the fit. The $I_0^{\ddagger}$ spectrum was calculated as the amplitude spectrum of the long time component in a fit of the 500 ps time scale data set and the I_1 spectrum was calculated as the final spectrum obtained on the 4 ns time scale. The sharp peak in the 470 nm region is a scattering artifact from the excitation beam.

sion). As the wavepacket moves away from the Franck-Condon region, the ground state bleaching partly recovers and the stimulated emission decays, due both to reformation of the ground state and to photochemical intermediate formation. The quantum efficiency of the photochemical process for the mutant is ~0.5, and agrees well with the value obtained for WT-PYP, as does the rate constant for I_0 formation. This indicates that the replacement of a carboxyl group by a carboxamide does not significantly alter the primary photochemistry, despite the fact that the hydrogen bonding between the chromophore hydroxyl and Glu64 is appreciably weakened by the mutation (as evidenced by the red shift in the absorption spectrum due to the increased anionic character of the phenolic oxygen).

In contrast, large rate constant differences (3- to 30-fold) between the mutant and WT-PYP are found in all of the subsequent photocycle transitions. This suggests that motions of the phenolic ring are involved in these steps, which can occur more easily because of the weakened H-bond, resulting in more rapid interconversion kinetics. Such movement apparently does not occur in the primary step (formation of I_0). This latter suggestion is in good agreement with the observation of Genick et al. (1998) that a rotation of the thioester carbonyl is the only structural change found in a PYP intermediate trapped at low temperature. In contrast, Perman et al. (1998) have reported motions of the phenolic ring occurring on the nanosecond time scale using Laue crystallography.

CONCLUSIONS

Femtosecond time-resolved spectroscopy has allowed us to characterize the excited state absorption, photoproduct appearance and relaxation, and ground state bleach and recovery processes for a Glu46Gln PYP mutant. On the femtosecond-to-picosecond time scale, intraprotein dynamics can be highly correlated. This property constitutes a fundamental difference with processes taking place on a longer time scale, where the dynamics are stochastic in nature. The structural differences that arise due to a change in the H-bonding between the carboxyl group (Glu46) and the amide group (Gln 46) and the chromophore anionic oxygen are seen to have important implications only for the relaxation of the protein occurring during the stages of the photocycle subsequent to the formation of the primary intermediate. As previously proposed (Genick et al., 1998), the thioester carbonyl in I_0 is in a distorted transition-state like conformation, highly constrained by the protein environment. In the Glu46Gln mutant, since the chromophore oxygen is more loosely held by the H-bond with the amide of Gln, there is more translational and vibrational freedom within the active site, and therefore the subsequent isomerization of the olefinic double bond can be essentially complete within 700 ps, as opposed to 3 ns for the WT protein. Further studies of the structural and mechanistic implica-

tions associated with additional mutations within the active site need to be undertaken in order to more fully understand the photophysical and photochemical processes occurring on these ultrafast time scales.

REFERENCES

Baca, M., G. E. O. Borgstahl, M. Boissinot, P. M. Burke, D. R. Williams, K. A. Slater, and E. D. Getzoff. 1994. Complete chemical structure of photoactive yellow protein: novel thioester-linked 4-hydroxycinnamyl chromophore and photocycle chemistry. *Biochemistry.* 33: 14369–14377.

Borgstahl, G. E. O., D. R. Williams, and E. D. Getzoff. 1995. 1.4 Å structure of photoactive yellow protein, a cytosolic photoreceptor: unusual fold, active site, and chromophore. *Biochemistry.* 34:6278–6287.

Chosrowjan, H., N. Mataga, Y. Shibata, Y. Imamoto, and F. Tokunaga. 1998. Environmental effects on the femtosecond-picosecond fluorescence dynamics of photoactive yellow protein: chromophores in aqueous solution and in protein nanospaces modified by site-directed mutagenesis. *J. Phys. Chem.* 102:7695–7698.

Devanathan, S., A. Pacheco, L. Ujj, M. Cusanovich, G. Tollin, S. Lin, and N. Woodbury. 1999. Femtosecond spectroscopic observations of initial intermediates in the photocycle of the photoactive yellow protein from *Ectothiorhodospira halophila*. *Biophys. J.* 77:1017–1023.

Genick, U. K., S. Devanathan, T. E. Meyer, I. L. Canestrelli, E. Williams, M. A. Cusanovich, G. Tollin, and E. D. Getzoff. 1997. Active site mutants implicate key residues for control of color and light cycle kinetics of photoactive yellow protein. *Biochemistry.* 36:8–14.

Genick, U. K., S. M. Soltis, P. Kuhn, I. L. Canestrelli, and E. D. Getzoff. 1998. Structure at 0.85 Å resolution of an early protein photocycle intermediate. *Nature.* 392:206–209.

Hoff, W. D., P. Dux, K. Hard, B. Devreese, I. M. Nugteren-Roodzant, W. Crielaard, R. Boelens, J. Van Beeuman, and K. J. Hellingwerf. 1994a. Thiol ester-linked p-coumaric acid as a new photoactive prosthetic group in a protein with rhodopsin-like photochemistry. *Biochemistry.* 33: 13959–13962.

Hoff, W. D., I. H. M. Van Stokkum, H. J. Ramesdonk, M. E. Van Brederode, A. M. Brouwer, J. C. Fitch, T. E. Meyer, R. Van Grondelle, and K. J. Hellingwerf. 1994b. Measurement and global analysis of the absorbance changes in the photocycle of the photoactive yellow protein from *Ectothiorhodospira halophila*. *Biophys. J.* 67:1691–1705.

Jiang, Z., L. R. Swem, B. G. Rushing, S. Devanathan, G. Tollin, and C. Bauer. 1999. Bacterial photoreceptor with similarity to photoactive yellow protein and plant phytochromes. *Science.* 285:406–409.

Meyer, T. E. 1985. Isolation and characterization of soluble cytochromes, ferredoxins and other chromophoric proteins from the halophilic phototrophic bacterium *Ectothiorhodospira halophila*. *Biochim. Biophys. Acta.* 806:175–183.

Meyer, T. E., E. Yakali, M. A. Cusanovich, and G. Tollin. 1987. Properties of a water-soluble, yellow protein isolated from a halophilic phototrophic bacterium that has photochemical activity analogous to sensory rhodopsin. *Biochemistry.* 26:418–423.

Meyer, T. E., G. Tollin, J. H. Hazzard, and M. A. Cusanovich. 1989. Photoactive yellow protein from the purple phototrophic bacterium *Ectothiorhodospira halophila*: quantum yield of photobleaching and effects of temperature, alcohols, glycerol and sucrose on kinetics of photobleaching and recovery. *Biophys. J.* 56:559–564.

Meyer, T. E., G. Tollin, T. P. Causgrove, P. Cheng, and R. Blankenship. 1991. Picosecond decay kinetics and quantum yield of fluorescence of the photoactive yellow protein from the halophilic purple phototrophic bacterium *Ectothiorhodospira halophila*. *Biophys. J.* 59:988–991.

Mihara, K., O. Hisatomo, Y. Imamoto, M. Katoaka, and F. Tokunaga. 1997. Functional expression and site-directed mutagenesis of photoactive yellow protein. *J. Biochem.* 121:876–880.

Perman, B., V. Rajer, Z. Ren, T. Teng, C. Pradervand, T. Ursby, F. Schotte, M. Wulff, R. Kort, K. J. Hellingwerf, and K. Moffat. 1998. Signal transduction on the nanosecond time scale: early structural events in the photocycle of a xanthopsin. *Science.* 279:1946–1950.

Sprenger, W. W., W. D. Hoff, J. P. Armitage, and K. J. Hellingwerf. 1993. The eubacterium *Ectothiorhodospira halophila* is negatively phototactic, with a wavelength dependence that fits the absorption spectrum of the photoactive yellow protein. *J. Bacteriol.* 175:3096–3104.

Ujj, L., S. Devanathan, T. E. Meyer, M. A. Cusanovich, G. Tollin, and G. H. Atkinson. 1998. New photocycle intermediates in the photoactive yellow protein from *Ectothiorhodospira halophila*: picosecond transient absorption spectroscopy. *Biophys. J.* 75:406–412.

Van Brederode, M. E., T. Gensch, W. D. Hoff, K. J. Hellingwerf, and S. E. Braslavsky. 1995. Photoinduced volume change and energy storage associated with the early transformations of the photoactive yellow protein from *Ectothiorhodospira halophila*. *Biophys. J.* 68:1101–1109.

Xie, A., W. D. Hoff, A. R. Kroon, and K. J. Hellingwerf. 1996. Glu 46 donates a proton to the 4-hydroxycinnamate anion chromophore during the photocycle of photoactive yellow protein. *Biochemistry.* 35: 14671–14678.